Radiation Physics and Chemistry 117 (2015) 83–87

Contents lists available at ScienceDirect

Radiation Physics and Chemistry

journal homepage: www.elsevier.com/locate/radphyschem

Evaluation of the medical and occupational shielding in cerebral angiography using Monte Carlo simulations and virtual anthropomorphic phantoms

William S. Santos [a,*], Lucio P. Neves [a,c], Ana P. Perini [a,c], Linda V.E. Caldas [a], Ana F. Maia [b]

[a] Instituto de Pesquisas Energéticas e Nucleares, Comissão Nacional de Energia Nuclear (IPEN-CNEN/SP), São Paulo, Brazil
[b] Departamento de Física, Universidade Federal de Sergipe, 49100-000 São Cristovão, SE, Brazil
[c] Instituto de Física, Universidade Federal de Uberlândia (INFIS/UFU), Caixa Postal 593, 38400-902, Uberlândia, MG, Brazil

HIGHLIGHTS

- Medical and occupational expositions during cerebral angiography exams were evaluated.
- This evaluation was undertaken employing Monte Carlo simulations.
- The evaluation was carried out by means of dose conversion coefficients (CCs).
- There was an increase of the CC values with the increase of the Al filtration.
- The results may be useful for reducing medical and occupational exposures.

ARTICLE INFO

Article history:
Received 15 September 2014
Accepted 22 July 2015
Available online 23 July 2015

Keywords:
Cerebral angiography
Dosimetry
Monte Carlo simulation

ABSTRACT

Cerebral angiography exams may provide valuable diagnostic information for the patients with suspect of cerebral diseases, but it may also deliver high doses of radiation to the patients and medical staff. In order to evaluate the medical and occupational expositions from different irradiation conditions, Monte Carlo (MC) simulations were employed. Virtual anthropomorphic phantoms (MASH) were used to represent the patient and the physician inside a typical fluoroscopy room, also simulated in details, incorporated in the MCNPX 2.7.0 MC code. The evaluation was carried out by means of dose conversion coefficients (CCs) for equivalent (H) and effective (E) doses normalized by the air kerma-area product (KAP). The CCs for the surface entrance dose of the patient (ESD) and equivalent dose for the eyes of the medical staff were determined, because CA exams present higher risks for those organs. The tube voltage was 80 kVp, and Al filters with thicknesses of 2.5 mm, 3.5 mm and 4.0 mm were positioned in the beams. Two projections were simulated: posterior–anterior (PA) and right-lateral (RLAT). In all situations there was an increase of the CC values with the increase of the Al filtration. The highest dose was obtained for a RLAT projection with a 4.0 mm Al filter. In this projection, the ESD/KAP and E/KAP values to patient were 11 (14%) mGy/Gy cm^2 and 0.12 (0.1%) mSv/Gy cm^2, respectively. For the physician, the use of shield lead glass suspended and lead curtain attached to the surgical table resulted in a significant reduction of the CCs. The use of MC simulations proved to be a very important tool in radiation protection dosimetry, and specifically in this study several parameters could be evaluated, which would not be possible experimentally.

1. Introduction

Cerebral angiography is a type of interventional procedure used for diagnose and to treat diseases of the central nervous system. In this type of procedure, radiographies are used for formation of medical images to guide the path of the catheter to the region of interest. This type of procedure increased significantly in recent years, and in large part, this is associated with the evolution of all technologies involved to perform complex interventional procedures. Beyond great benefits, it can cause high doses to the physician and the patient, because usually high fluoroscopy times are

* Corresponding author. Fax: +55 11 3133 9678.
E-mail addresses: wssantos@ipen.br (W.S. Santos), lucio.neves@ufu.br (L.P. Neves), anapaula.perini@ufu.br (A.P. Perini), lcaldas@ipen.br (L.V.E. Caldas), afmaia@ufs.br (A.F. Maia).

http://dx.doi.org/10.1016/j.radphyschem.2015.07.014
0969-806X/

required (Alexander et al., 2010). However, there are a few dosimetric studies that investigated the radiation levels that these individuals are exposed to.

To evaluate the medical and occupational exposures it is necessary to know accurately the absorbed doses in organs and tissues of individuals. However, a direct estimation of the doses is complicated, and even impossible in most situations. In this sense, new methodologies need to be adopted, and the Monte Carlo simulation is one of the most reliable methods for interventional radiology procedures (Santos et al., 2014). In this approach, the representation of exposed individuals is made by using an anthropomorphic phantom incorporated to a radiation transport code. The results of the doses of organs and tissues of the phantom are shown in terms of conversion coefficients (CCs), which are obtained as the ratio of a dosimetric quantity (measured or estimated) by a measured quantity as air kerma-area product (KAP) or the entrance skin dose (ESD). In this sense, some studies have been done in radiology and interventional cardiology. Ferrari et al. (2010), Bozkurt and Bor (2007) and Santos et al. (2014) used pairs of anthropomorphic phantoms and the MCNPX code to estimate CCs for equivalent and effective doses of patients and physicians in interventional radiology procedures. The results of CCs published in these studies were determined for anatomical regions and X-ray tube projections different from those of brain procedures.

The main objective of this study is to develop a simulation scenario to determine the CCs of equivalent and effective doses to patients and physicians using the most frequent technical parameters in cerebral angiography procedures. The main contribution of this research is the use of anthropomorphic phantoms standing and lying, which represent with more reliability the positions of the patient and the physician in a cerebral procedure.

Another feature of this research was the detailed description of the procedure room and personal protective equipment. They allowed the evaluation of the efficiency of the lead curtain and suspended protectors of glass mixed with lead. Besides, an evaluation of CCs to equivalent dose to the eye lens of the physician and ESD for patient were carried out. The evaluation of ESD and equivalent dose in eye lens is one of the most important aspects of radiological protection (Fletcher et al., 2002; Moritake et al., 2008). These quantities provide valuable information about the possible deterministic effects.

2. Materials and methods

To estimate the doses to organs and tissues of the patient and the physician in a cerebral angiography procedure, Monte Carlo simulations were performed using the radiation transport code MCNPX (Pelowitz, 2011). This code can handle the transport and interactions of photons, electrons, neutrons and other particles for a wide range of energy, employing three-dimensional geometric surfaces. The patient and the physician were each one represented by an adult anthropomorphic phantom named MASH (*Male Adult meSH*) (Cassola et al., 2010). These phantoms have more than 100 organs and tissues with significance for dosimetry. They represent an adult with 1.76 m height, 72.7 kg of body mass, employing voxels with an edge of 0.24 cm length each one. They were built on the basis of anatomical and anthropometric data suggested by the ICRP 89 (2002).

The advantage of using these phantoms is that each one was constructed in two positions, lying and standing, allowing the actual representation of the patient and the physician. Thus, some of the anatomical defects caused by the gravitational force as the displacement of the internal organs of the chest cavity, compression of the lungs, reduction of sagittal diameter, changes in the position of the arms and shoulders in the dorsal direction, and cranial displacements were taken into consideration. In this way, it is expected that the results of CCs, utilizing these phantoms, are more accurate than those obtained with mathematical phantoms, developed utilizing mathematical equations, or those obtained with voxel phantoms, which were developed employing computed tomography and magnetic resonance images, obtained with the patient lying down.

All main components available in the room where cerebral angiography procedures are performed were modeled in the computational framework to simulate the radiation transport. The room has 6.5 m in length, 3.0 m wide and 2.65 m height filled with atmospheric air ($\rho = 0.001205$ g/cm^3). The composition of the atmospheric air was C (0.0124%), N (75.53%), O (23.18%) and Ar (1.28%). The concrete walls ($\rho = 3.2$ g/cm^3) were built with 0.22 m in thickness. Inside this room, besides the physician and the patient, the main components of an X-ray equipment were added, such as the image intensifier and X-ray tube ($\rho = 11.35$ g/cm^3; composition: Pb (100%)). A surgical table was modeled employing carbon fiber ($\rho = 1.25$ g/cm^3; composition: H (5.7441%), C (77.4591%), O (16.7968%)) with a width of 66.0 cm, a thickness of 15.0 cm and a length of 185.0 cm, positioned 90.0 cm from the floor. The physician was positioned on the left side of the surgical table, at shoulder level of the patient, and in front of the video monitor system, as can be seen in Fig. 1.

The X-ray tube and its metal base can be moved to simulate the usual angled projections of cerebral angiography procedures. Fig. 1 shows the exposure computational model with the phantoms representing the patient (lying on the surgical table) and the physician positioned on the side of the surgical table using a lead apron, thyroid shield and lead glasses. All these equipment are 0.5 mm Pb thick, in a typical configuration of cerebral angiography. A lead curtain attached to the surgical table and a suspended glass shield, both with an equivalent thickness of 0.5 mm lead, are also visible in Fig. 1. They are intended to protect the medical professionals from the primary radiation beam, and especially, the scattered radiation from the patient and the surgical table. These new equipment protections are better shown in Fig. 2.

The X-ray tube was simplified to a point source emitting photons isotropically in a solid angle, specified by the field size and the focal distance. The ionization chamber that is coupled to the output of the majority of X-ray equipment was also added to the simulation. It was modeled as an object with 3 cm × 3 cm in size and a thickness of 1 cm, filled with atmospheric air, and used to calculate the KAP. This object was positioned on the X-ray tube output, as shown in Fig. 2(a). The KAP was determined as the product of the air kerma (K_{air}) (obtained by *tally F6*) by the

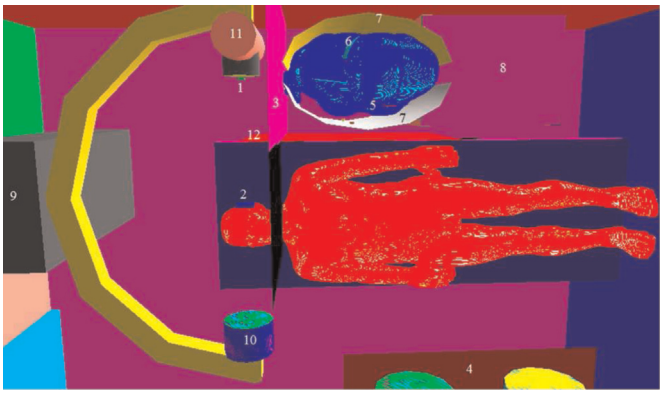

Fig. 1. Main components of a room of cerebral angiography procedures: (1) KAP measure system; (2) ESD measure system; (3) suspended shield lead glass; (4) video monitors, (5) lead glasses; (6) thyroid shield; (7) lead apron; (8) table for the surgical instrumentation; (9) X-ray equipment; (10) image intensifier; (11) X-ray tube and (12) lead curtain attached to the surgical table.

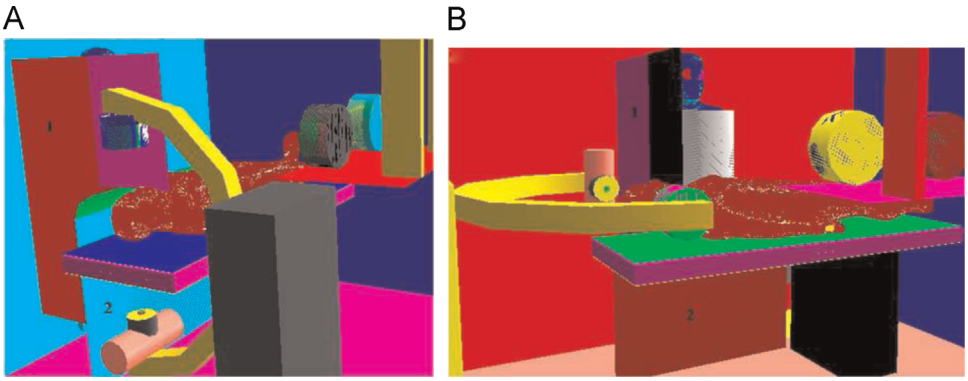

Fig. 2. Visualization of the projection PA (a), lateral RLAT (b) and the lead curtain attached to the surgical table (2) (in a and b) and shield lead glass suspended (1) (in a and b).

irradiated area of the ionization chamber, which is considered equivalent to the irradiated area of the patient. In this research the KAP was determined for the two studied projections (PA and RLAT).

In order to evaluate the possible deterministic effects, an object that simulates an ionization chamber with dimensions of the radiation field (7 cm × 7 cm) was inserted in the simulation, to calculate the ESD of the patient. In all projections, the ionization chamber was placed next to the skin of the patient and perpendicular to the central axis of the radiation beam. The estimated ESD of the patient was determined using the MCNPX *F6 tally*. The absorbed dose in the organ was calculated by the product of the total energy deposited in the organ (in MeV obtained by the ∗*F8 tally*) over the corresponding mass of the organ/tissue (in kg).

In this study, the spectra used in the simulation were generated with the software SRS 78 (Cranley et al., 1997). The radiographic parameters most frequently used in cerebral angiography procedures were obtained from the literature (Siiskonen et al., 2007). The values of these radiographic parameters were a beam filtration of 2.5, 3.5 and 4.0 mmAl, an anode angle of 12° and a tube voltage of 80 kVp. Other parameters used in the simulations were an area of radiation field of 7 cm × 7 cm, a focus-to-skin distance of 44 cm in the posterior–anterior projection (PA) and 64 cm on the right-lateral projection (RLAT). In order to reduce the statistical uncertainties associated with the absorbed dose, 10^9 histories were used in each scenario. All simulations were performed using a computer with 16 GB of RAM and an Intel Core i7 processor.

3. Results and discussion

The main CC values for the equivalent (H) and effective (E) doses for the physician, and the values of H, E, and the entrance skin dose (ESD) to the patient are shown in Tables 1 and 2, respectively. These CCs were calculated for the main organs and radiosensitive tissues recommended by ICRP 103 (2007). For the physician, the results are presented for two exposure scenarios. In scenario I the lead curtain attached to the surgical table and the shield suspended glass were not used, and in scenario II, these protective equipment were used (highlighted parts of Table 1).

An important observation should be made regarding the use of a lead curtain attached to the surgical table and the suspended protective shield lead glass. Their use protects the physician from the scattered radiation (mainly from the patient), which consequently leads to lower CC values for equivalent and effective doses.

The reductions among the CCs for effective dose, given in Table 1, for the physician were 6.7, 6.5 and 6.7, respectively, for the PA projections with 2.5, 3.5 and 4.0 mmAl, and 4.2, 6.7 and 3.3, for the RLAT projections, respectively. In Table 1, it is also possible to observe that a reduction of the CCs for equivalent dose to the eye lens of the physician reached values of 2.5, 3.3 and 3.2 for PA projections, and 25, 16 and 15 for RLAT projections, respectively. Thus, these differences reinforce the importance of using the lead curtain and the lead glass suspended protectors. Otherwise, the dose threshold for cataract formation could be achieved in a few years (Vano et al., 2008). In all studied scenarios, the highest values of CCs for equivalent dose of the physician were calculated for red bone marrow, bone surface, brain, remainder organs and eye lenses.

The average of CCs for effective dose, on the physician, with a beam filtration of 2.5, 3.5 and 4.0 mmAl calculated for scenario II were 3.5E−02, 3.2E−02 and 4.8E−02 mSv/Gy cm^2, respectively. These values were compared with experimental studies in cardiac procedures. Padovani and Rodella (2001) calculated CCs for effective doses to different groups of interventional physicians, and they found a mean value of 0.23 μSv/Gy cm^2. Tsapaki et al. (2004) estimated 0.132 and 0.168 μSv/Gy cm^2 to effective dose in procedures for coronary angiography and percutaneous transluminal coronary angioplasty, respectively. Bor et al. (2006) evaluated the doses of nine physicians in five different coronary angiography rooms and obtained an average value of 0.14 μSv/Gy cm^2. All these values are higher than those presented in this study. The main reason can be attributed to a large energy absorption by the bone material from the patient's head and that were targeted in the primary beam of the X-rays.

As expected, and demonstrated, the majority of the critical organs of the patient, located in or near the field of vision (FOV), were the most irradiated ones. They are red bone marrow, thyroid, bone surface, brain, salivary glands and eye lenses. These organs obtained high CCs for equivalent dose when compared to distant organs, located far from the primary radiation field, i.e., colon, stomach, gonads, bladder and liver, which are affected only by the scattered radiation. The average CCs for the effective dose to the patient with beam filtrations of 2.5, 3.5 and 4.0 mmAl were 6.7E−02, 7.6E−02 and 8.2E−02 mSv/Gy cm^2, respectively. These results show, respectively, differences of 23%, 13% and 6% compared to the value 8.7E−02 mSv/Gy cm^2 published by NCRP 160 for cerebral angiography procedures (NCRP 160, 2009).

CCs for the equivalent dose of skin, presented by this study, should be used only to estimate the effective dose. In real situations, only a small portion of the patient's skin is directly irradiated by the beam. Due to the possibility of acute symptoms of radiation, the CCs for ESD presented in this study consider the information about the location and dimensions of the radiation field and in this sense it is believed that it is the best option to evaluate the possibility of deterministic effects to the patient. CCs to ESD of patients calculated in the two projections are shown in Table 2. Note the differences between the evaluated projections.

Table 1
CCs to H and E normalized by KAP in μSv/Gy cm^2 for the physician using three types of beam filtration. The statistical uncertainties (%) are in parentheses. The highlighted parts represent the scenarios where the protective equipment were employed.

Organs	PA			RLAT		
	2.5 mmAl	3.5 mmAl	4.0 mmAl	2.5 mmAl	3.5 mmAl	4.0 mmAl
Red bone marrow	7.9E-01(0.1)	9.3E-01(0.1)	9.9E-01(0.1)	4.7E-01(0.1)	4.7E-01(0.1)	5.5E-01(0.1)
	1.1E-01(0.1)	1.3E-01(0.1)	1.4E-01(0.1)	3.6E-02(0.1)	4.6E-02(0.1)	4.9E-02(0.1)
Colon	3.1E-02(0.4)	3.7E-02(0.4)	3.8E-02(0.4)	2.4E-02(0.3)	2.4E-02(0.3)	3.1E-02(0.3)
	2.5E-03(0.1)	2.8E-03(0.1)	2.9E-03(0.1)	2.0E-02(0.1)	2.4E-02(0.3)	2.5E-02(0.3)
Lung	3.4E-02(0.2)	4.2E-02(0.2)	4.3E-02(0.2)	2.4E-02(0.1)	2.4E-02(0.1)	2.9E-02(0.2)
	8.9E-03(0.1)	1.3E-02(0.1)	1.4E-02(0.1)	6.6E-03(0.4)	8.7E-03(0.1)	1.0E-02(0.2)
Stomach	5.0E-02(0.7)	6.2E-02(0.8)	7.3E-02(0.9)	4.1E-02(0.5)	4.1E-02(0.5)	5.1E-02(0.6)
	6.7E-03(0.3)	6.8E-03(0.1)	6.9E-03(0.3)	2.2E-02(0.7)	3.4E-02(0.5)	3.8E-02(0.6)
Breast	2.2E-02(2.6)	2.5E-02(1.1)	3.9E-02(1.3)	1.6E-02(0.7)	1.6E-02(0.7)	2.3E-02(1.6)
	3.2E-03(0.3)	6.0E-03(0.2)	6.8E-03(0.4)	1.0E-02(0.9)	1.7E-02(1.0)	2.6E-02(0.7)
Gonads	2.4E-02(0.9)	2.8E-02(1.4)	3.0E-02(1.3)	2.6E-02(0.9)	2.6E-02(0.9)	4.1E-02(0.9)
	2.1E-03(0.1)	2.5E-03(0.4)	2.7E-03(0.1)	2.3E-02(0.6)	3.4E-02(1.1)	2.7E-02(0.1)
Bladder	1.6E-02(0.6)	2.8E-02(0.9)	3.6E-02(1.1)	1.6E-02(0.6)	1.6E-02(0.6)	1.9E-02(0.6)
	1.9E-04(0.1)	8.6E-04(0.5)	4.1E-03(0.4)	1.4E-02(0.4)	1.3E-02(0.5)	1.4E-02(1.5)
Oesophagus	1.6E-02(0.6)	2.8E-02(0.8)	3.0E-02(0.8)	2.5E-02(0.8)	2.5E-02(0.8)	4.6E-02(0.7)
	5.5E-03(0.5)	8.3E-03(0.1)	9.2E-03(0.4)	6.4E-03(0.1)	1.7E-02(0.6)	3.4E-02(0.3)
Liver	2.1E-02(0.1)	2.6E-02(0.2)	2.9E-02(0.2)	9.0E-03(0.1)	9.0E-03(0.1	1.5E-02(0.1)
	1.9E-03(0.1)	3.1E-03(0.4)	3.2E-03(0.1)	5.3E-03(0.9)	8.3E-03(0.1)	9.1E-03(0.3)
Thyroid	5.1E-02(1.6)	7.0E-02(2.0)	1.3E-01(2.9)	4.2E-02(1.3)	4.2E-02(1.3)	6.9E-02(1.5)
	1.9E-02(1.1)	3.7E-02(0.1)	5.4E-02(1.8)	1.9E-02(0.1)	3.5E-02(1.3)	2.6E-02(1.4)
Bone surface	1.7E+00(0.8)	2.0E+00(0.9)	2.2E+00(0.9)	1.1E+00(0.6)	1.1E+00(0.6)	1.3E+00(0.3)
	2.4E-01(0.3)	2.8E-01(1.4)	3.1E-01(0.4)	8.0E-02(0.1)	9.9E-02(0.2)	1.1E-01(0.2)
Brain	3.4E-01(0.6)	4.1E-01(0.7)	4.4E-01(0.7)	3.3E-01(0.5)	3.3E-01(0.5)	4.0E-01(0.3)
	1.0E-01(0.3)	1.3E-01(0.3)	1.4E-01(0.4)	2.4E-02(0.5)	3.5E-02(0.2)	3.6E-02(3.5)
Salivary glands	4.4E-01(2.0)	5.4E-01(1.7)	5.7E-01(1.7)	1.3E+00(3.4)	1.3E+00(3.4)	1.4E+00(1.4)
	1.4E-01(0.9)	1.45-01(0.4)	1.8E-01(1.0)	1.2E-01(0.1)	1.5E-01(0.6)	1.7E-01(3.4)
Skin	5.5E-01(0.4)	6.3E-01(0.5)	6.7E-01(0.5)	3.1E-01(0.3)	3.1E-01(0.3)	3.5E-01(0.2)
	4.9E-02(0.1)	5.6E-02(1.0)	6.0E-02(0.2)	2.1E-02(0.1)	2.7E-02(0.1)	2.8E-02(0.2)
Remainder organs	5.5E-01(4.8)	7.0E-01(5.5)	7.5E-01(5.6)	3.7E-01(4.0)	3.7E-01(0.2)	4.6E-01(3.5)
	9.3E-02(1.2)	9.9E-02(1.3)	1.0E-01(1.4)	1.6E-01(1.9)	2.0E-01(0.1)	2.4E-01(0.2)
Eye lens	3.7E+00(7.1)	5.0E+00(9.1)	5.5E+00(7.5)	3.2E+00(6.3)	3.2E+00(3.5)	3.5E+00(5.8)
	1.5E+00(4.7)	1.5E+00(4.8)	1.7E+00(3.7)	1.3E-01(1.2)	2.0E-01(3.6)	2.3E-01(4.0)
Effective dose	2.2E-01(0.7)	2.6E-01(0.7)	2.8E-01(0.7)	1.5E-01(0.5)	1.6E-01(0.2)	1.8E-01(0.5)
	3.3E-02(0.2)	4.0E-02(0.2)	4.2E-02(0.2)	3.6E-02(0.3)	2.4E-02(0.2)	5.4E-02(0.3)

Table 2
CCs for H, E and ESD normalized by KAP in mSv/Gy cm^2 for the patient using three types of beam filtration. The statistical uncertainties (%) are in parentheses.

Organs	PA			RLAT		
	2.5 mmAl	3.5 mmAl	4.0 mmAl	2.5 mmAl	3.5 mmAl	4.0 mmAl
Red bone marrow	1.3E−01(0.2)	1.6E−01(0.2)	1.7E−01(0.1)	4.3E−01(0.2)	4.8E−01(0.1)	5.0E−01(0.1)
Colon	5.5E−05(0.1)	7.1E−05(0.1)	8.1E−05(0.0)	3.2E−05(0.0)	3.3E−05(0.1)	3.9E−05(0.0)
Lung	5.7E−03(0.0)	6.8E−03(0.0)	7.3E−03(0.0)	1.9E−03(0.0)	2.3E−03(0.0)	2.4E−03(0.0)
Stomach	3.8E−04(0.0)	4.9E−04(0.0)	5.2E−04(0.0)	1.8E−04(0.0)	2.5E−04(0.0)	2.6E−04(0.0)
Breast	7.7E−04(1.2)	8.2E−04(1.0)	9.1E−04(1.0)	8.5E−04(1.0)	1.1E−03(1.1)	1.2E−03(1.0)
Gonads	7.5E−05(1.2)	5.0E−05(1.2)	4.4E−05(1.0)	3.6E−05(1.0)	4.0E−05(0.6)	2.4E−05(0.5)
Bladder	2.5E−05(1.1)	4.3E−05(1.0)	3.2E−05(0.8)	4.9E−06(0.4)	7.3E−06(0.2)	8.7E−06(0.1)
Oesophagus	5.8E−03(0.7)	7.2E−03(0.2)	7.9E−03(0.2)	1.9E−03(0.1)	2.4E−03(0.1)	2.5E−03(0.1)
Liver	5.1E−04(0.1)	6.2E−04(0.1)	6.8E−04(0.1)	2.0E−04(0.2)	2.5E−04(0.1)	2.8E−04(0.1)
Thyroid	1.7E−02(0.1)	2.1E−02(0.1)	2.3E−02(0.2)	9.3E−03(0.2)	1.1E−02(0.1)	1.2E−02(0.1)
Bone surface	3.5E−01(1.2)	4.0E−01(1.1)	4.2E−01(1.0)	1.1E+00(1.0)	1.2E+00(1.0)	1.3E+00(1.0)
Brain	4.2E−01(1.3)	5.0E−01(0.6)	5.3E−01(0.4)	1.2E+00(0.8)	1.4E+00(0.5)	1.5E+00(0.5)
Salivary glands	8.2E−02(0.2)	9.8E−02(0.3)	1.1E−01(0.2)	4.7E−01(0.2)	5.2E−01(0.1)	5.5E−01(0.1)
Skin	3.0E−02(0.4)	3.4E−02(0.3)	3.6E−02(0.4)	7.8E−02(0.5)	8.1E−02(0.4)	8.2E−02(0.3)
Remainder organs	7.5E−02(0.4)	8.9E−02(0.4)	9.7E−02(0.4)	1.7E−01(0.8)	1.9E−01(1.1)	2.1E−01(1.3)
Eye lens	2.7E−02(0.2)	3.2E−02(0.2)	3.6E−02(0.2)	4.7E+00(2.2)	5.0E+00(2.4)	5.1E+00(2.5)
Effective dose	3.5E−02(0.1)	4.1E−02(0.1)	4.4E−02(0.1)	9.9E−02(0.2)	1.1E−01(0.1)	1.2E−01(0.1)
Entrance skin dose	4.2E+00(9.3)	4.6E+00(10)	4.9E+00(10)	9.8E+00(12)	1.0E+01(13)	1.1E+01(14)

When the X-ray tube is below the surgical table (PA projection), it attenuates the beam and the main results are CCs with lower values, relative to the lateral-projection (RLAT) where the X-ray tube is located slightly above the surgical table.

As may be observed in Tables 1 and 2, the obtained CCs presented high values with the increase of the beam filtration. For the specific conditions studied, i.e., increasing the beam filtration, it was possible to observe a decrease in KAP, implying in the increase of the CCs equivalent dose to organs and tissues evaluated, resulting in higher effective dose to the studied individuals. Apart from modifications to the beam filtration, the results show the influence of beam projection on the individual exposure stating that these operational aspects are largely responsible for the increase of CCs.

4. Conclusions

From the analysis of the results, it is possible to demonstrate and quantify the increase of CCs for equivalent and effective doses as a result of the increase of the beam filtration. In addition to the apron, thyroid shield and lead glasses, the results clearly show the importance of using the lead curtain attached to the surgical table and the suspended shield lead glass. These protective equipment with an equivalent thickness of 0.5 mm of lead reduced on average the CCs for equivalent dose in the eye lens and effective dose to physician for maximum factors of 25 and 6.7, respectively. It may be concluded that the use of PA projection reduces the average CCs for ESD for the patient by a factor of 2.3. The results presented in this study may be useful for reducing medical and occupational exposure of individuals involved in cerebral angiography procedures.

Acknowledgments

The authors of this paper received support from the Brazilian agencies São Paulo Research Foundation (FAPESP, Grant nos. 2013/15669-3 and 2013/21741-9), CAPES (Project Pró-estratégia no. 1999/2012), CNPq and INCT (Project INCT for Radiation Metrology in Medicine nos. 2008/57863-2 and 573659/2008-7).

References

Alexander, M.D., Oliff, M.C., Olorunsola, O.G., Brus-Ramer, M., Nickoloff, E.L., Meyers, P.M., 2010. Patient radiation exposure during diagnostic and therapeutic interventional neuroradiology procedures. J. NeuroIntervent. Surg. 2, 6–10.

Bor, D., Onal, E., Olgar, T., Caglan, A., Toklu, T., 2006. Measurement and estimation of cardiologist dose received in interventional examinations. In: AAPM 48th Annual Meeting, Orange County Convention Center Orlando, FL, USA, July 30–August 3.

Bozkurt, A., Bor, D., 2007. Simultaneous determination of equivalent dose to organs and tissues of the patient and of the physician in interventional radiology using the Monte Carlo method. Phys. Med. Biol. 52, 317–330.

Cassola, V.F., de Melo Lima, V.J., Kramer, R., Khoury, H.J., 2010. FASH and MASH: Female and Male Adult human phantoms based on polygon meSH surfaces. Part I: development of the anatomy. Phys. Med. Biol. 55, 133–162.

Cranley, K., Gilmore, B.J., Fogarty, G.W.A., Desponds, L., 1997. Catalogue of Diagnostic X-Ray Spectra and Other Data. Institute of Physics and Engineering in Medicine, Report 78, IPEM, York.

Ferrari, P., Venture, G., Gualdrini, G., Rossi, P.L., Marriseli, M., Zannoli, R., 2010. Evaluation of the dose to the patient and medical staff in interventional cardiology employing computational models. Radiat. Prot. Dosim. 141, 82–85.

Fletcher, D.W., Miller, D.L., Balter, S., Taylor, M.A., 2002. Comparison of four techniques to estimate radiation dose to skin during angiographic and interventional radiology procedures. J. Vasc. Interv. Radiol. 13, 391–397.

ICRP 89, 2002. Basic Anatomical and Physiological Data for Use in Radiological Protection Reference Values. ICRP Publication 89. Ann. ICRP 32 (3–4).

ICRP 103, 2007. The 2007 Recommendations of the International Commission on Radiological Protection. ICRP Publication 103. Ann. ICRP 37 (2–4).

Moritake, T., Matsumaru, Y., Takigawa, T., Nishizawa, K., Matsumura, A., Tsuboi, K., 2008. Dose measurement on both patients and operators during neurointerventional procedures using photoluminescence glass dosimeters. Am. J. Neuroradiol. 29, 1910–1917.

NCRP 160, 2009. Ionizing Radiation Exposure of the Population of the United States. Report 160, Bethesda, MD.

Padovani, R., Rodella, C.A., 2001. Staff dosimetry in interventional cardiology. Radiat. Prot. Dosim. 94, 99–103.

Pelowitz, D.B., 2011. MCNPX User's Manual, Version 2.7.0. Report LA-CP-11-00438. Los Alamos National Laboratory.

Santos, W.S., Carvalho Jr., A.B., Hunt, J.G., Maia, A.F., 2014. Using the Monte Carlo technique to calculate dose conversion coefficients for medical professionals in interventional radiology. Radiat. Phys. Chem. 95, 177–180.

Siiskonen, T., Tapiovaara, M., Kosunen, A., Lehtinen, M., Vartiainen, E., 2007. Monte Carlo simulations of occupational radiation doses in interventional radiology. Br. J. Radiol. 80, 460–468.

Tsapaki, V., Kottou, S., Patsilinakos, S., Voudris, V., Cokkinos, D.V., 2004. Radiation dose measurements to the interventional cardiologist using an electronic personal dosemeter. Radiat. Prot. Dosim. 112, 245–249.

Vano, E., Gonzalez, L., Fernández, J.M., Haskal, Z.J., 2008. Eye lens exposure to radiation in interventional suites: caution is warranted. Radiology 248, 945–953.